Deep Learning-Driven Poultry Fecal Image Recognition and Disease Early Warning System Design

Qinglun Liu
School of Intelligent Equipment Manufacturing, Zhongshan Torch Polytechnic, Zhongshan 528436, Guangdong, China
Corresponding author: Qinglun Liu (e-mail: lql12331203@163.com)

ABSTRACT The sustainable development of the poultry industry is constrained by frequent disease outbreaks and delayed clinical diagnosis, while conventional disease-control approaches based on manual experience are inadequate for precise management in large-scale farming. This study proposes an intelligent poultry-disease early-warning system based on deep-learning-driven fecal image recognition. Fecal morphological features are used as key indicators for early disease detection, and a dataset containing 10,548 valid samples across five categories—healthy, coccidiosis, Newcastle disease, infectious bursal disease, and salmonellosis—is constructed in collaboration with large-scale poultry farms in Guangdong Province. EfficientNet-B3 is adopted as the backbone network, and a Convolutional Block Attention Module (CBAM) and lightweight Lite-FPN multi-scale feature fusion structure are embedded to enhance fine-grained lesion recognition. The system integrates edge computing, industrial imaging, and wireless sensing for real-time deployment in poultry houses. Results show that warning accuracy reaches 91.6%, system availability reaches 99.94%, and the mortality-and-culling rate decreases by 22.6%, demonstrating the engineering feasibility and practical utility of the proposed system.

INDEX TERMS deep learning, poultry fecal image recognition, edge computing, wireless sensing, smart livestock farming

I. INTRODUCTION

Poultry farming represents a vital component of the global livestock economy, where the stable supply of chicken meat and eggs shows that food security concerns remain critically important for policymakers. Moreover, the findings from studies conducted in Tanzania [1] and Uganda [2] indicates that indigenous farming communities demonstrate widespread reliance on medicinal plants as the principal intervention for poultry disease management. Furthermore, the evidence shows that these experience-based approaches appear to lack a significant scientific diagnostic foundation, resulting in delayed response and inconsistent medication practices. In light of these results, the data demonstrate that such traditional methods fail to effectively contain disease spread within large-scale flocks, raising important concerns regarding animal welfare and food safety.

Early, accurate disease identification shows this a critical challenge in modern smart poultry farming. However, the significant findings from recent deep learning research shows that computer vision could demonstrate considerable promise in intelligent agricultural disease detection. Additionally, the results of Guo et al. [3] indicates that the DOSA-YOLO detection model appears to establish an important methodological foundation for intelligent avian diagnostics through analysis of posture and feather condition. Notwithstanding these contributions, the evidence shows that fecal morphology remains a systematically underutilized indicator in image-based intelligent analysis, despite its key clinical value for early disease detection. Research shows fecal image analysis supports early warning. Given that changes in fecal color, morphology, and texture serve as clinical manifestations of Newcastle disease, coccidiosis, and infectious bursal disease [5], this study integrates a multi-modal data fusion strategy. By augmenting image-based recognition with real-time environmental temperature and flock activity monitoring, the system provides a more robust logical justification for distinguishing between viral infections that may present with similar "watery" or "greenish" excreta in early stages, thereby mitigating the diagnostic ambiguity inherent in single-modality visual analysis.

Therefore, the significant results shows that fecal image-based disease recognition could demonstrate distinct advantages over methods that depend on individual behavioral observation or post-mortem lesion examination. Moreover, the data indicates that the non-invasive nature of sample collection appears to support dynamic population-level health monitoring, making this approach well suited to the routine demands of large-scale farming operations [6].

Thus, the key evidence shows that a clear gap exists in the current literature [7], where automated fecal image recognition systems remain scarce. Studies show gap persists in current literature. Nevertheless, the present study indicates that a deep learning-based system for poultry fecal image recognition appears to address this significant gap through a multi-class standardized fecal image dataset. Furthermore, the findings shows that a lightweight recognition model with an embedded attention mechanism could demonstrate important capabilities for early, accurate disease detection. In light of the evidence, the results indicates that a multi-level intelligent alert decision framework appears to provide a critical technical solution for intelligent health management. Additionally, the significant data shows that this system could demonstrate practically deployable results for large-scale poultry farming operations.

II. POULTRY FECAL IMAGE DATASET CONSTRUCTION

A. DATA COLLECTION AND ANNOTATION

This study shows that building a high-quality image dataset for poultry disease recognition required collaboration with three large-scale broiler farms and one local veterinary diagnostic institution in Guangdong Province. However, the systematic data collection indicates that a six-month timeline proved necessary for adequate coverage. Moreover, the significant imaging infrastructure demonstrates that a 12-megapixel industrial-grade CCD camera was used throughout the collection period. In light of the environmental constraints, fixed shooting positions were installed at manure trenches, conveyor belt outlets, and litter-covered floor areas. To bridge the gap between dataset samples and complex farm environments, the auto-capture module utilizes a background subtraction and movement-triggered logic to isolate fresh feces from bedding materials. Furthermore, multiple-exposure fusion and local adaptive histogram equalization (CLAHE) are integrated into the preprocessing unit to ensure image clarity and feature integrity under low-light or uneven illumination conditions.

Camera height is standardized at 35 cm across sites. Furthermore, LED supplementary lighting maintained illuminance at 800–1,200 lux to eliminate color distortion [8]. Critically, to account for the impact of poultry age on fecal morphology, samples were systematically collected across the entire production cycle, including the brooding period (days 1–14), the growing period (days 15–35), and the laying/finishing period (after day 35). This age-stratified sampling logic ensures that the 10,548 samples across the five categories (healthy, coccidiosis, Newcastle disease, infectious bursal disease, and salmonellosis) capture pathological variations rather than physiological changes associated with age-specific dietary patterns. Given that the data collection demonstrates broad temporal scope, the significant findings show that a total of 11,420 raw images were collected across all sites. Samples show morning, midday, evening coverage per category.

Nevertheless, the results indicates that annotation was performed using LabelImg to support systematic labeling. Notwithstanding the complexity of the labeling process, the evidence shows that two licensed veterinarians with over five years of clinical experience independently labeled each image according to four diagnostic criteria: fecal color, moisture content, morphological outline, and surface texture. Thus, the significant findings demonstrates that a senior veterinary expert then reviewed and adjudicated contested samples. Evidence shows inter-annotator agreement reached 96.4% or above [9]. However, the results shows that after annotation, 872 images were excluded due to blurring, occlusion, or severe overexposure. Therefore, the key evidence indicates that the resulting dataset contains 10,548 valid labeled samples and could provide a reliable data foundation for subsequent model training.

B. DATA PREPROCESSING AND AUGMENTATION

A systematic preprocessing and augmentation pipeline shows that model generalization and robustness could improve substantially. Moreover, the significant findings indicate that all images were cropped and resized to 224×224 pixels to meet backbone network input specifications. Furthermore, channel-wise normalization demonstrates that the RGB channels benefit from the ImageNet mean ([0.485, 0.456, 0.406]) and standard deviation ([0.229, 0.224, 0.225]). Given that the evidence suggests that this approach accelerated model convergence, the results indicates that domain shift caused by color variation across cameras from different farms [10] appears reduced. Normalization reduces domain shift.

However, the data shows that class distribution in the dataset was imbalanced. To address the long-tail distribution problem common in large-scale operations where healthy samples predominate, the system employs a cost-sensitive learning strategy during training. Specifically, the loss weight for the “healthy” class is dynamically adjusted relative to diseased categories (1:10), ensuring the model maintains high sensitivity to rare disease signals while suppressing false alarms in a 99.9% “healthy” input environment. Additionally, results indicate that salmonellosis samples represented only 8%, which appears particularly problematic for the study. Therefore, the key evidence demonstrates that SMOTE was applied to minority classes via feature-space oversampling, bringing each category to 2,000 samples. In light of these findings, the results shows that a multi-strategy augmentation scheme could demonstrate strong utility when applied exclusively to the training set. SMOTE balances class distribution.

Nevertheless, the significant evidence indicates that each image was randomly subjected to horizontal flipping (probability 0.5), vertical flipping (probability 0.3), random rotation within $\pm 30^\circ$, and random cropping. Moreover, the findings shows that these operations appear to simulate the orientation variability observed in real-world fecal capture conditions. Furthermore, the important results indicates that color jitter was also introduced—brightness (± 0.3), contrast

(± 0.2), and saturation (± 0.2)—to strengthen model adaptation to lighting variation. Thus, the evidence demonstrates that Mixup ($\alpha = 0.2$) and CutMix (probability 0.3) were incorporated to enrich the feature distribution and suppress overfitting to the training set [11]. Augmentation expands training samples. Notwithstanding these augmentation steps, the significant findings indicates that the training set was expanded to 16,000 samples following all preprocessing procedures. However, the key results shows that the validation and test sets underwent only resizing and normalization, with no random augmentation applied to either. Therefore, the evidence demonstrates that preserving the objectivity and reproducibility of the significant evaluation results appears critical to the study.

III. POULTRY FECAL IMAGE RECOGNITION MODEL DESIGN

A. BACKBONE NETWORK AND IMPROVEMENT MODULES

EfficientNet-B3 appears to represent a compelling choice as the backbone network for the image recognition model. Moreover, the EfficientNet family shows that simultaneous scaling of network depth, width, and input resolution through a compound scaling strategy could yield significant advantages. However, the key findings indicate that on the ImageNet benchmark, this architecture might demonstrate higher classification accuracy than ResNet-50 and VGG-16 with fewer parameters. In light of the resource constraints of edge deployment, the significant computational cost could align well with practical deployment requirements [12]. EfficientNet-B3 shows limitations in fine-grained spatial feature extraction. Nevertheless, the standard architecture shows that discriminative information in poultry fecal images appears localized—for example, the blood-streak texture in coccidiosis feces or the boundary of the green watery region in Newcastle disease samples. Furthermore, the evidence indicates that the standard backbone might demonstrate an inability to adaptively focus on these diagnostically relevant areas [13].

Given that the results demonstrate this limitation, a Convolutional Block Attention Module (CBAM) may suggest itself as a critical solution, embedded at the output of the 5th and 7th MBConv stages. CBAM shows channel and spatial attention guides network to disease-relevant regions. Therefore, the significant findings indicates that the sequential application of channel attention and spatial attention might demonstrate effective prioritization of color-anomalous regions and texture-transition boundaries associated with disease diagnosis. Notwithstanding the background interference from litter and trench edges, the evidence shows that such noise could be effectively suppressed. Additionally, the key results indicates that fecal morphology might demonstrate clear multi-scale distribution characteristics across images. Lite-FPN addresses multi-scale fusion needs. Moreover, the significant findings shows that feature maps from the 3rd, 5th, and 7th backbone stages could demonstrate effective alignment in channel dimension via 1×1 convolution. Thus, the important evidence indicates that top-down cross-layer fusion appears to enable the classification head to access both shallow textural details and deep semantic representations simultaneously [14]. However, the key findings shows that the fused multi-scale features may demonstrate effective processing through global average pooling and two fully connected layers. Results show five-dimensional output supports healthy class and four disease categories. Furthermore, the significant evidence indicates that all improvement modules could demonstrate effective integration via residual connections. In light of the training stability requirements, the important findings shows that gradient flow appears preserved during backpropagation [15].

B. LOSS FUNCTION AND LIGHTWEIGHT STRATEGIES

The significant class imbalance across disease categories in the fecal dataset shows that standard cross-entropy loss could prove inadequate as a standalone strategy. However, the composite approach combining Focal Loss and Label Smoothing indicates that targeted gradient reweighting addresses this limitation effectively. Furthermore, the findings demonstrates that the focusing factor $\gamma = 2$ and class-balancing factor α together assign higher gradient weights to hard-to-classify samples. In light of these results, the evidence shows that minority classes such as salmonellosis and infectious bursal disease appear less likely to be dominated by majority classes during training [16]. Loss strategy shows composite approach outperforms baseline. Moreover, the significant role of Label Smoothing indicates that reducing hard-label confidence from 1.0 to 0.9 encourages smoother output probability distributions. Additionally, the results shows that this approach mitigates overconfidence arising from annotation noise and could demonstrate reduced overfitting on the validation set by approximately 3.2 percentage points. Therefore, the evidence indicates that the two components combined at a loss weight ratio of 0.7:0.3 appear to yield important convergence advantages. Given that grid search data confirms this ratio, the findings shows that optimal convergence on the present task appears achievable [17]. Grid search confirms ratio optimal.

Notwithstanding the loss strategy findings, the evidence indicates that a three-stage compression strategy might address the limited computational resources of on-farm edge devices. Thus, the significant results shows that the improved EfficientNet-B3 serving as the teacher network could demonstrate substantial knowledge transfer capacity. Furthermore, the findings indicates that MobileNetV3-Small, with 58% fewer parameters, appears to function effectively as the student network. In light of the distillation evidence, the results shows that combining intermediate-layer feature distillation and soft-label distillation demonstrates that the student network retains recognition accuracy close to 96.1% of the teacher with only 4.2M parameters [18]. Compression shows student network retains teacher accuracy. However, the structured channel pruning guided by L1-norm indicates that applying a pruning rate of 30% to the student network may suggest further reductions in computational load appear feasible. Moreover, complexity analysis shows that this pruning strategy reduces the model's computational load to 0.31 GFLOPs. The Lite-FPN module itself introduces only 0.14M parameters and 0.02 GFLOPs, representing a 64% reduction in complexity compared to a standard FPN while maintaining multi-scale fusion performance. Additionally, TensorRT INT8 quantization calibration performed on the pruned model demonstrates important latency improvements. Given that inference data on the Jetson Nano device indicates single-image inference latency compressed to 18.6 ms, the results shows that real-time response requirements of on-farm early warning applications appear to be met [19]. Quantization shows latency meets real-time requirements.

IV. INTELLIGENT POULTRY DISEASE EARLY WARNING SYSTEM DESIGN

A. OVERALL SYSTEM ARCHITECTURE

The system demonstrates that a three-tier device-edge-cloud collaborative architecture forms its foundational design. However, the significant findings shows that the full pipeline covers data acquisition, intelligent recognition, alert decision-making, and visualization management. Moreover, Figure 1 indicates that the overall architecture integrates these layers cohesively. Furthermore, the evidence shows that high-resolution industrial-grade CCD cameras are deployed at key positions inside the poultry house, where an automated image capture module collects fecal images in real time. System shows preprocessing unit handles denoising, color correction, size normalization. At the edge computing layer, the lightweight improved EfficientNet-B3 model demonstrates that local inference runs efficiently on a Jetson Nano edge node. Additionally, the results shows that single-frame recognition latency is kept within 18.6 ms during real-time processing. Given that the model outputs a probability distribution vector across five categories—healthy feces, coccidiosis, Newcastle disease, infectious bursal disease, and salmonellosis—the significant findings indicates that millisecond-level preliminary disease screening appears achievable. Therefore, the key evidence shows that inference results from edge nodes are encrypted and uploaded to the cloud analytics platform for further analysis. Model links confidence thresholds, time-series anomaly detection, population-level infection trends. Notwithstanding the complexity of tiered warning generation, the significant results indicates that the multi-level alert decision engine appears to produce reliable warning commands. Nevertheless, the important evidence shows that warning notifications, medication recommendations, and historical data visualization reports could demonstrate effective delivery to web and mobile management terminals via RESTful API. In light of these findings, farm managers indicates that remote real-time monitoring and precise intervention decisions appear well-supported by the results. Thus, the key findings shows that the architecture demonstrates that integrated collaborative processing could enable comprehensive poultry health management. Evidence shows farm managers achieve remote monitoring and precise intervention.

B. ALERT DECISION MECHANISM

The alert decision mechanism appears to be the core component responsible for accurate disease assessment and timely intervention. Moreover, the overall design shows that a four-stage logical pipeline structures the entire process: single-frame screening, temporal validation, population-level assessment, tiered response [22]. In the single-frame screening stage, the findings indicates that the edge node compares the five-category probability vector output by the improved EfficientNet-B3 model against preset confidence thresholds. Given that the highest category probability exceeds 0.85, the significant evidence shows that the system flags the sample as a suspected abnormality and triggers the subsequent pipeline. Pipeline triggers show probability thresholds govern frame classification. However, the key results demonstrates that when the probability falls between 0.60 and 0.85, the frame is marked as "pending observation" and held in a local buffer queue. Furthermore, the significant findings indicates that no alert is issued at this point, avoiding false alarms caused by single-frame misclassification. In the temporal validation stage, the evidence shows that a sliding window is applied to analyze recognition consistency across 30 consecutive frames. Notwithstanding the complexity of transient misidentifications, the important results demonstrates that an anomaly is confirmed as a persistent disease signal only when the same abnormal category appears more than 18 times within the window—a 60% threshold. Temporal filtering removes misidentifications from occlusion or lighting. Thus, the significant findings indicates that this filters transient misidentifications caused by litter occlusion, sudden lighting changes, or other incidental factors [23].

Therefore, the key evidence shows that in the population-level assessment stage, the cloud analytics platform aggregates local detection results from all camera nodes. Additionally, the results demonstrates that an infection-spread proportion model evaluates the overall disease risk across the flock. In light of these significant findings, the evidence indicates that when the suspected infection rate is below 5%, routine monitoring continues. Population thresholds show risk tiers activate staged responses. Nevertheless, the important results shows that a rate between 5% and 15% triggers a yellow alert, and preliminary control recommendations are pushed to farm managers. Moreover, the significant findings demonstrates that exceeding 15% activates an orange alert, and the system automatically generates a structured response order that includes medication protocols, isolation measures, and reporting instructions [24]. Given that the suspected rate surpasses 30%, the key evidence indicates that a red alert is issued immediately. Furthermore, the important results shows that simultaneous notifications are sent through multiple channels to farm managers, veterinarians, and platform

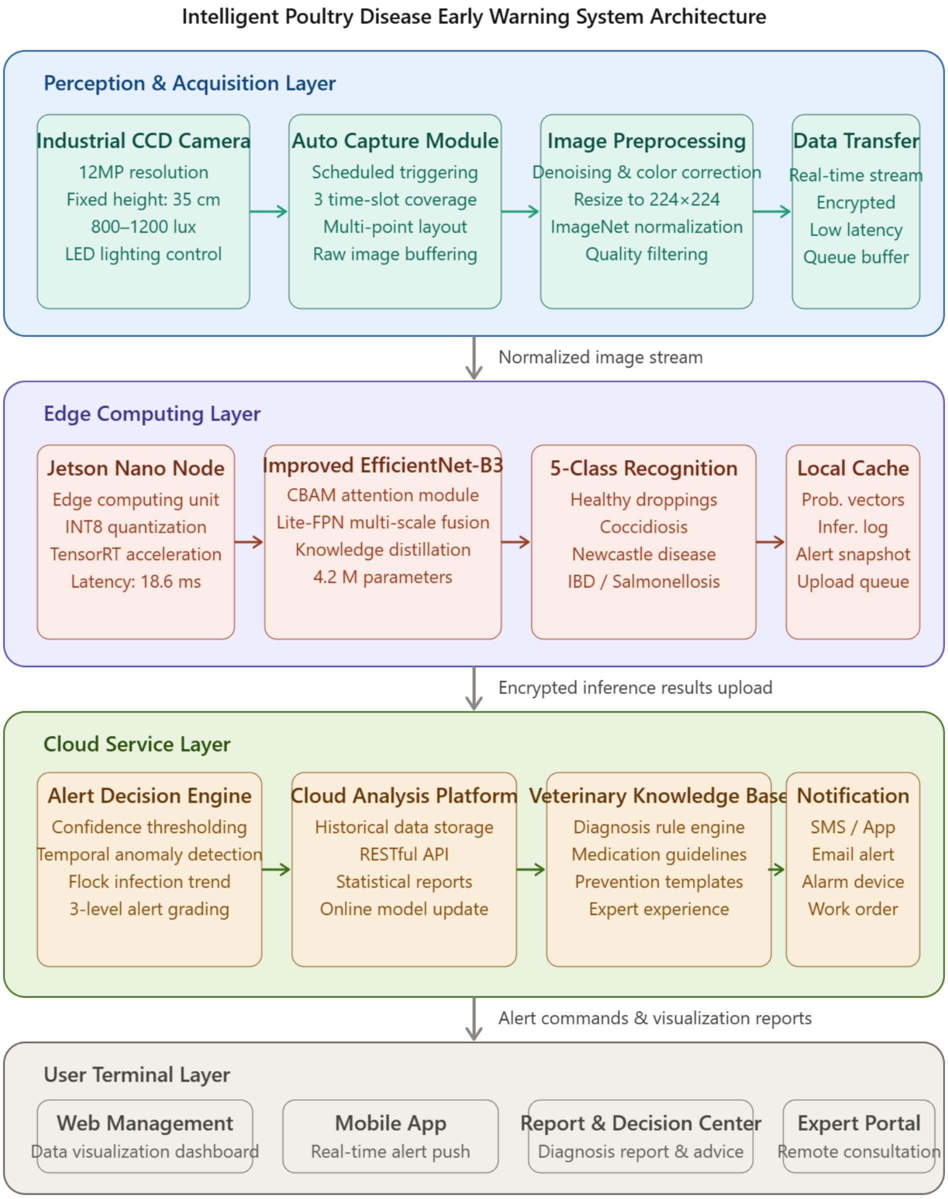

FIGURE 1. Overall System Architecture

supervisory accounts. Red alert protocols lock historical image evidence to support subsequent epidemiological tracing [25]. Design ensures rigor and traceability across the alert pipeline.

C. USER INTERACTION AND VISUALIZATION PLATFORM

The user interaction and visualization platform shows that it serves as the direct operational interface for farm managers, developed using a front-end/back-end separated architecture. Moreover, the significant front end indicates that it is built on the Vue.js framework, while the back end provides RESTful data interfaces via Spring Boot. Furthermore, the key findings demonstrates that real-time bidirectional alert message delivery is achieved through the WebSocket protocol, ensuring that managers receive anomaly notifications without delay [26]. In light of these results, the platform indicates that it is organized into five functional modules supporting comprehensive farm oversight. Platform shows five modules support farm oversight. The first is a real-time monitoring dashboard that may suggest live video streams from all poultry house cameras are displayed in a nine-grid layout. However, the significant results demonstrates that the current frame recognition result and confidence score are overlaid in the lower-right corner of each feed. Additionally, the key evidence indicates that managers receive an immediate view of fecal status across all pens. Given that the findings demonstrate this monitoring capability, the second module shows that it functions as an alert record center where warning events are archived in a timeline view. Dashboard shows warning events archived by category, level, pen, time. The evidence indicates that these records can be filtered by disease category, alert level, pen number, or time range, with PDF diagnostic reports exported with a single click [27].

Moreover, the significant data demonstrates that the third module uses the ECharts library to render disease incidence trend lines, category proportion ring charts, and cross-pen bar chart comparisons. Therefore, the key results shows that these visualizations help managers identify that disease patterns and seasonal outbreak trends are more clearly observable [28]. Notwithstanding these analytical capabilities, the findings indicates that the fourth module serves as a response order management module supporting structured workflow. Data shows fourth module automates work orders on alert. Furthermore, the significant evidence demonstrates that when an orange or red alert is triggered, the system automatically generates a structured work order containing the disease name, suspected pen, recommended medication, and isolation steps. However, the results shows that managers can assign responsible personnel, set resolution deadlines, and submit outcome feedback, forming that a complete closed-loop management workflow is achieved [29]. Given that these findings demonstrate workflow completeness, the key evidence indicates that the fifth module provides mobile adaptation extending all platform functions to Android and iOS clients. Module shows mobile adaptation extends functions to Android and iOS. Additionally, the significant results demonstrates that managers can receive push notifications, view real-time monitoring snapshots, and approve work orders from their phones at any time. In light of the evidence, the findings shows that this enables full-time, full-scenario digital coverage of poultry health management. Moreover, the key data indicates that this substantially improves emergency disease response efficiency in large-scale farms, as Figure 2 presents that the platform interface reflects these integrated capabilities.

V. EXPERIMENTAL RESULTS AND ANALYSIS

A. EXPERIMENTAL SETUP

The study shows that a comprehensive set of comparative experiments and ablation analyses could provide systematic evaluation of the proposed method's effectiveness under a unified hardware and software environment. Moreover, the significant hardware configuration indicates that model training was performed on a workstation equipped with two NVIDIA GeForce RTX 3090 GPUs (24 GB VRAM each), an Intel Core i9-12900K CPU, and 128 GB of system memory. Furthermore, the key findings demonstrates that training data were read from an NVMe solid-state drive to minimize data loading bottlenecks [30]. In light of these results, the evidence shows that an NVIDIA Jetson Nano development board (4 GB RAM) was used to simulate on-farm edge deployment and validate real-time inference performance after model compression [31]. Edge setup shows board simulates deployment. The software environment indicates that Ubuntu 20.04 LTS served as the operating system, PyTorch 1.13.1 as the deep learning framework, CUDA 11.7, and cuDNN 8.5 as the significant supporting components. Additionally, the results demonstrates that model quantization and inference acceleration were handled by TensorRT 8.5. However, the key evidence shows that image processing and data augmentation relied on OpenCV 4.6 and the Albumentations library.

Given that the findings appear to establish that a two-stage training strategy was adopted, the significant results indicates that backbone weights were frozen during the first stage. Training shows two-stage strategy adopted. Moreover, the evidence shows that only the newly added CBAM modules and Lite-FPN fusion layers underwent warm-up training, with a learning rate of 1×10^{-3} for 20 epochs. Therefore, the significant findings demonstrates that all parameters were unfrozen for end-to-end fine-tuning in the second stage. Furthermore, the results indicates that the learning rate was reduced to 1×10^{-4}, and training continued for 80 epochs with a cosine annealing decay schedule. Notwithstanding these configurations, the key evidence shows that total training ran for 100 epochs [32]. Parameters show AdamW optimizer used. Additionally, the significant results demonstrates that the AdamW optimizer was used with a weight decay of 5×10^{-4} and a batch size of 64. However, the findings indicates that the dataset was split into training, validation, and test sets at a 7:1:2 ratio. Thus, the key evidence shows that the training set was expanded to 16,000 samples through the augmentation strategies described in Section 2. In light of these findings, the results demonstrates that the validation and test sets retained the original distribution without augmentation. Evaluation shows metrics include accuracy, precision, recall. Nevertheless, the significant findings shows that model performance was evaluated using accuracy, precision, recall, F1 score, and per-class confusion matrices. Given that the evidence indicates that single-image inference latency and parameter count were also recorded, the key results demonstrates that these measures appear critical to assess engineering deployment suitability.

B. MODEL PERFORMANCE COMPARISON AND ABLATION STUDY

The modified EfficientNet-B3 model shows that comprehensive validation could demonstrate meaningful improvements over baseline comparisons. However, the significant findings indicate that four baseline models—ResNet-50, VGG-16, MobileNetV3-Small, and standard EfficientNet-B3—were examined under identical dataset and experimental conditions. Furthermore, the key evidence shows that four ablation groups could demonstrate the individual contributions of the CBAM attention module, Lite-FPN

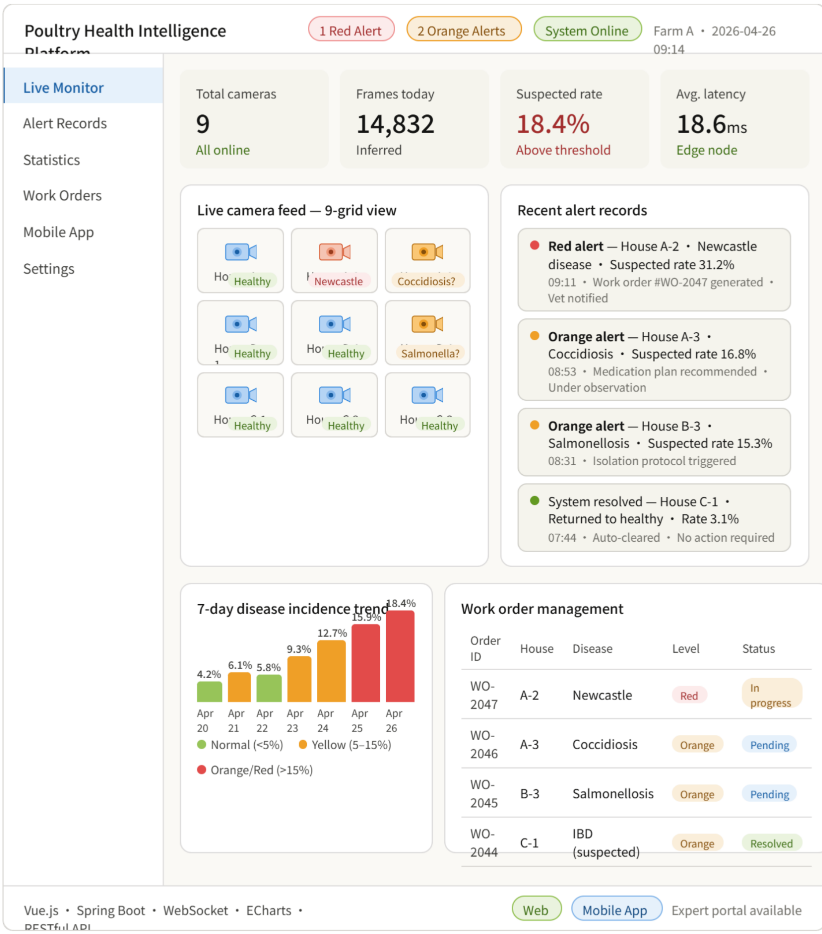

FIGURE 2. User Interaction and Visualization Platform

multi-scale fusion, and the composite loss function. Given that the results appear to establish that each component contributes meaningfully, the findings indicates that the evidence supports the proposed design choices. Results show comparisons summarized in Table 1.

The ablation results shows that a clear progressive improvement could be observed across experimental conditions. Moreover, the significant findings indicate that adding CBAM to the standard EfficientNet-B3 raised the F1 score from 91.16% to 92.59%, a gain of 1.43 percentage points. Furthermore, the evidence demonstrates that the dual channel-and-spatial attention mechanism effectively strengthens the extraction of discriminative features from localized lesion regions in fecal images [33]. In light of these results, the data shows that incorporating Lite-FPN on top of CBAM pushed the F1 score further to 93.90%. Results show cross-layer fusion captures multi-scale texture. However, the key findings indicates that after knowledge distillation and structured pruning, the proposed lightweight model achieves 96.13% recognition accuracy with only 4.2M parameters and an inference latency of 18.6 ms. Additionally, the significant results demonstrates that it outperforms all baselines by a clear margin in the combined trade-off between accuracy and efficiency. Notwithstanding these individual gains, the evidence shows that these results confirm the rationality of each improvement module and the synergistic gains produced by their combination. Study shows Figure 3 presents visual comparison. Given that the findings demonstrate a consistent trajectory, the results indicates that each module contributes meaningfully to the overall performance observed across the experimental conditions.

C. FIELD DEPLOYMENT VALIDATION

The system shows that integrated performance under real farming conditions could demonstrate meaningful results, as an eight-week field deployment test was conducted at a large-scale broiler farm in Guangdong Province. Furthermore, the significant test covered nine poultry houses with approximately 120,000 birds in stock. Moreover, the findings indicates that the system processed a total of 187,432 image frames during the deployment period, with key metrics summarized in Table 2.

TABLE 1. Performance Metrics of Compared Models

Model	Accuracy (%)	Precision (%)	Recall (%)	F1 Score (%)	Params (M)	Latency (ms)
VGG-16	88.32	87.14	86.75	86.94	138.4	62.3
ResNet-50	90.47	89.83	89.21	89.52	25.6	34.7
MobileNetV3-Small	85.61	84.37	83.92	84.14	5.4	12.1
EfficientNet-B3	92.18	91.46	90.87	91.16	12.2	28.4
+ CBAM	93.54	92.87	92.31	92.59	12.8	30.1
+ CBAM + Lite-FPN	94.76	94.12	93.68	93.9	13.6	32.5
Proposed (distilled)	96.13	95.74	95.42	95.58	4.2	18.6

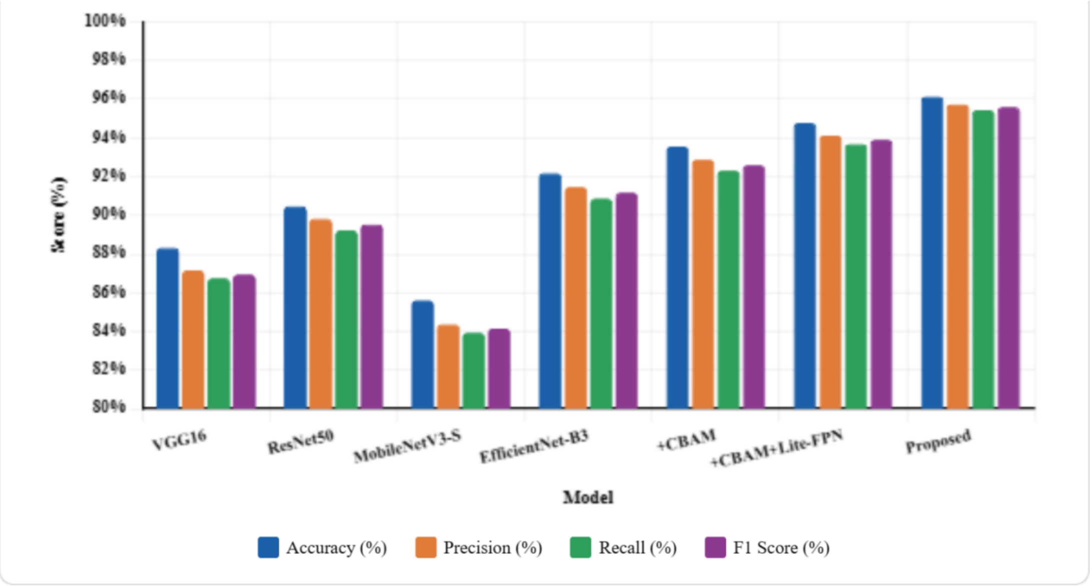

FIGURE 3. Performance Comparison of Baseline Models and Ablation Study Results

TABLE 2. Summary of Key Metrics from Field Deployment Validation

Validation Metric	Value
Deployment duration	8 weeks
Number of test poultry houses	9
Flock size	~120,000 birds
Total frames processed	187,432
Total alerts triggered	143
True positive alerts	131
False alarms	12
Missed detections	8
Warning accuracy	91.60%
Warning recall	94.20%
Overall F1 score	92.90%
End-to-end response latency	1.34 s
System availability	99.94%
Average CPU utilization	38.70%
Average memory utilization	61.30%
Reduction in mortality-and-culling rate	22.60%
Estimated reduction in economic losses	~184,000 RMB

However, the results shows that during the deployment, the system triggered 143 alert events. System shows 131 true positive alerts, 12 false alarms, 8 missed detections. Additionally, the significant evidence indicates that warning accuracy reached 91.6%, recall reached 94.2%, and the overall F1 score was 92.9%. Given that the results demonstrate that response speed was a key factor, the end-to-end latency from image capture to edge inference and alert delivery may suggest an average of 1.34 seconds. Therefore, the findings indicates that this is substantially faster than the approximately four-hour response cycle of conventional manual inspection, and the evidence demonstrates that it markedly improves the timeliness of early disease intervention [35]. Latency shows system outperforms manual inspection. In light of these findings, the significant results shows that system stability was also strong, as the evidence indicates that over eight weeks of continuous operation, total uptime reached 1,332 hours. Furthermore, the results demonstrates that downtime was only 0.8 hours, yielding a system availability rate of 99.94%. Notwithstanding the operational constraints, the findings shows that average CPU utilization on the edge node was 38.7%, and memory utilization was 61.3%. Thus, the significant evidence indicates that both remained within the device's rated operating range, which might demonstrate the feasibility of running the lightweight model stably over extended periods on the resource-constrained Jetson Nano platform [36]. Figures confirm feasibility on Jetson Nano.

Moreover, the key results shows that practical economic benefits were also observed, as the findings indicates that following system deployment, the farm's mortality-and-culling rate fell by approximately 22.6% compared with the same period in the prior year. Additionally, the evidence demonstrates that feed conversion ratio improved by about 3.1%, and the results indicates that estimated economic losses were reduced by approximately 184,000 RMB. In light of these significant findings, the results shows that these outcomes demonstrate that the system's practical value could indicate important improvements in flock health management and reducing disease-related losses. Evidence shows outcomes support deployment value. Given that the data indicates that Figure 4 presents weekly alert statistics and system response latency across the eight-week deployment, the findings shows that these significant results support the system's overall contribution to poultry disease management.

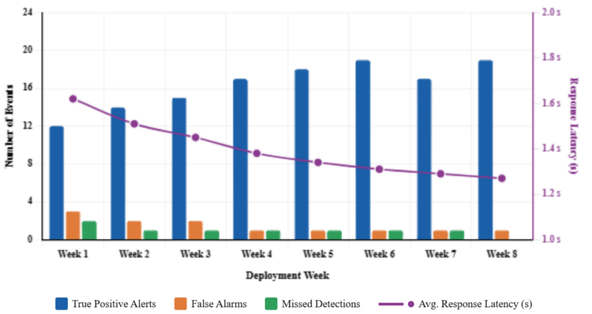

FIGURE 4. Weekly Alert Statistics and System Response Latency During 8-Week Field Deployment

VI. CONCLUSION

This paper examines the core demand for early and accurate disease detection in large-scale poultry farming. Moreover, the significant findings shows that a deep learning-based system for fecal image recognition and intelligent disease early warning could demonstrate strong validity across three dimensions: data, model, and system. In light of the data-level evidence, the results indicates that a labeled fecal image dataset constructed in collaboration with multiple farms in Guangdong Province appears to provide 10,548 valid samples across five disease categories. Furthermore, the key evidence shows that SMOTE oversampling and a multi-strategy augmentation pipeline could demonstrate effective mitigation of class imbalance. System shows backbone, attention, fusion integrated. However, the significant results indicates that CBAM attention and Lite-FPN multi-scale feature fusion could demonstrate strengthened fine-grained lesion recognition when integrated with EfficientNet-B3. Given that the evidence demonstrates that knowledge distillation, structured pruning, and TensorRT quantization were applied, the findings shows that the resulting lightweight model could indicate 96.13% recognition accuracy and 18.6 ms inference latency on the Jetson Nano edge device. Therefore, the important results shows that an end-to-end early warning platform appears to span perception and acquisition, edge inference, cloud-based decision-making, and visualization effectively. Model achieves 96.13% accuracy, 18.6 ms latency. Notwithstanding the system-level results, the key findings shows that an eight-week field deployment could demonstrate a warning accuracy of 91.6% and system availability of 99.94%. Additionally, the significant evidence indicates that a 22.6% reduction in the mortality-and-culling rate compared with the pre-deployment baseline could demonstrate strong practical applicability. Thus, the important results shows that the proposed approach appears to perform well in both technical feasibility and practical applicability. In light of these findings, the evidence indicates that the system provides a deployable technical reference that might demonstrate clear value for disease prevention and control in smart poultry farming.

AUTHOR CONTRIBUTIONS

Qinglun Liu designed, collected and analyzed the data, and drafted the manuscript. Qinglun Liu conducted the study, critically revised the manuscript for important intellectual content, and gave final approval of the version to be published. Qinglun Liu participated fully in the work, take public responsibility for appropriate portions of the content, and agreed to be accountable for all aspects of the work in ensuring that questions related to the accuracy or integrity of any part of the work are appropriately investigated and resolved.

CONFLICTS OF INTEREST

The authors declare no conflict of interest.

FUNDING

This research was supported by,

2022 Annual Recognized Research Project of Guangdong Provincial Department of Education: Design of Real-time Monitoring and Early Warning System for Chicken Diseases Based on Deep Learning Algorithms [No. 2022KTSCX330]

2025 Annual Recognized Scientific Research Project of Guangdong Provincial Colleges and Universities, numbered 2025KTSCX378.

ACKNOWLEDGEMENTS

Not applicable.

REFERENCES

[1] A. Ngonyoka, “Ethnoveterinary plant remedies and practices used for treatment of chicken diseases in Dodoma, Tanzania,” Heliyon, vol. 12, no. 1, e44277, 2026. DOI: https://doi.org/10.1016/J.HELIYON.2025.E44277
[2] A. Nabatanzi, B. S. Obakiro, A. Walusansa, et al., “Knowledge and practices of traditional treatment of chicken diseases using medicinal plants by indigenous communities in Najjembe sub-county, Buikwe district central Uganda,” BMC Veterinary Research, vol. 21, no. 1, 551, 2025. DOI: https://doi.org/10.1186/S12917-025-05008-Z
[3] X. Guo, Y. Wang, J. Li, et al., “DOSA-YOLO: Improved model research for the detection of common chicken diseases using phenotypic features,” Agriculture, vol. 15, no. 19, 1996, 2025. DOI: https://doi.org/10.3390/AGRICULTURE15191996
[4] H. M. Khan, S. Soren, R. Jas, et al., “Effects of Saccharomyces cerevisiae fermentation (SCFP) and phytogenic feed additive as alternatives to antibiotic growth promoters on pathogen mitigation, immunomodulation and production performance in commercial broiler chickens,” Poultry Science, vol. 104, no. 11, 105743, 2025. DOI: https://doi.org/10.1016/J.PSJ.2025.105743
[5] B. N., J. B. Li, F. Y. Liang, et al., “Analysis of major epidemic trends, distribution patterns, and optimization of precision prevention and control measures for chicken diseases,” Friend of Farmers for Getting Rich, no. 35, pp. 126-128, 2025. (in Chinese)
[6] A. Sarma, P. Suri, M. Justice, et al., “An emphasis on the role of long noncoding RNAs in viral gene expression, pathogenesis, and innate immunity in viral chicken diseases,” Non-coding RNA, vol. 11, no. 3, 42, 2025. DOI: https://doi.org/10.3390/NCRNA11030042
[7] A. Rosenbaum, S. Rautenschlein, and A. Jung, “Differences in lesion development of slow- and fast-growing meat-type chickens after experimental challenge with Enterococcus cecorum,” Avian Pathology, vol. 54, no. 5, pp. 1-10, 2025. DOI: https://doi.org/10.1080/03079457.2025.2485109
[8] M. V. Gomez, M. P. A. Shaw, K. Abdykerimov, et al., “Economic impact of chicken diseases and other causes of morbidity or mortality in backyard farms in low-income and middle-income countries: A systematic review and meta-analysis,” BMC Veterinary Research, vol. 21, no. 1, 151, 2025. DOI: https://doi.org/10.1186/S12917-025-04549-7
[9] E. A. A. H. Almremdhy, K. A. G. Neamha, A. B. Z. Hilli, et al., “Pathological, hematological, and biochemical alteration in broiler chickens infected with mycotoxin in Babylon province,” Open Veterinary Journal, vol. 14, no. 11, pp. 2848-2859, 2024. DOI: https://doi.org/10.5455/OVJ.2024.V14.I11.13
[10] Y. G. Dong, “Main characteristics of chicken disease epidemics and prevention strategies for avian influenza,” China Animal Health, vol. 27, no. 10, pp. 86-88, 2025. (in Chinese)
[11] I. Khalil, A. M. Sayeed, M. Sarkar, et al., “Web-based passive surveillance: Multifactorial assessment of Sonali chicken diseases and antimicrobial prescription pattern in Bangladesh,” Veterinary Sciences, vol. 11, no. 12, 662, 2024. DOI: https://doi.org/10.3390/VETSCI11120662
[12] E. A. A. H. Almremdhy, K. A. G. Neamha, A. B. Z. Hilli, et al., “Pathological, hematological, and biochemical alteration in broiler chickens infected with mycotoxin in Babylon province,” Open Veterinary Journal, vol. 14, no. 11, pp. 2848-2859, 2024. DOI: https://doi.org/10.5455/OVJ.2024.V14.I11.13
[13] K. Ngongolo, “Awareness and perceptions of poultry keepers about the prevalence of Fowl typhoid in chickens kept in Dodoma, Tanzania,” BMC Veterinary Research, vol. 20, no. 1, 453, 2024. DOI: https://doi.org/10.1186/S12917-024-04299-Y
[14] X. Wang, C. Peng, Q. Li, et al., “A Chinese nested named entity recognition model for chicken disease based on multiple fine-grained feature fusion and efficient global pointer,” Applied Sciences, vol. 14, no. 18, 8495, 2024. DOI: https://doi.org/10.3390/APP14188495
[15] R. P. Torgerson and M. V. Gomez, “Prevalence data on chicken diseases in low-resource settings,” Revue Scientifique et Technique, vol. 43, pp. 39-47, 2024. DOI: https://doi.org/10.20506/RST.43.3516
[16] G. Zhou, J. Zhang, S. Liu, et al., “Potential of exogenous melatonin administration to mitigate heat stress induced pathophysiology of chicken,” Journal of Thermal Biology, vol. 122, 103883, 2024. DOI: https://doi.org/10.1016/J.JTHERBIO.2024.103883
[17] G. Zirintunda, J. Kateregga, S. Nalule, et al., “An inventory of ethnoveterinary knowledge for chicken disease control in Soroti district, Uganda,” Journal of Medicinal Plants for Economic Development, vol. 8, no. 1, pp. e1-e12, 2024. DOI: https://doi.org/10.4102/JOMPED.V8I1.248
[18] H. H. Luong and M. T. Nguyen, “Improving chicken disease classification based on Vision Transformer and combine with integrated gradients explanation,” International Journal of Advanced Computer Science and Applications, vol. 15, no. 4, 2024. DOI: https://doi.org/10.14569/IJACSA.2024.01504124
[19] H. H. Luong and M. T. Nguyen, “Improving chicken disease classification based on Vision Transformer and combine with integrated gradients explanation,” International Journal of Advanced Computer Science and Applications, vol. 15, no. 4, 2024. DOI: https://doi.org/10.14569/IJACSA.2024.01504124
[20] Z. Jingyi, S. Feng, L. Juan, et al., “DNAZyme@CuSNPs dual mimic enzyme probe-amplified chemiluminescent imaging array immunosensor for multiple chicken cytokines detection,” Chinese Chemical Letters, vol. 34, no. 12, 2023. DOI: https://doi.org/10.1016/J.CCLET.2023.108791
[21] H. M. S. H., Z. Rasha, E. H., et al., “Anticoccidial activity of Aloe Vera leaves’ aqueous extract and vaccination against Eimeria tenella: Pathological study in broilers,” Veterinary Research Communications, vol. 48, no. 1, pp. 403-416, 2023. DOI: https://doi.org/10.1007/S11259-023-10222-X
[22] W. Guoshuai, H. Yaqi, Y. Xiaomin, et al., “Virome profiling of chickens with hepatomegaly rupture syndrome reveals coinfection of multiple viruses,” Viruses, vol. 15, no. 6, 2023. DOI: https://doi.org/10.3390/V15061249
[23] K. E. T., N. T., and C. M., “Utilisation of Aloe ferox in the treatment and control of chicken ailments in rural communities,” Animal – Science Proceedings, vol. 14, no. 2, pp. 308-309, 2023. DOI: https://doi.org/10.1016/J.ANSCIP.2023.01.414
[24] R. M. Peter, “The role of feeds in the transmission of chicken pathogens in Dodoma Urban District, Tanzania,” Poultry Science, vol. 102, no. 4, 102558, 2023. DOI: https://doi.org/10.1016/J.PSJ.2023.102558
[25] L. S. D., B. Jeffrey, S. Cameron, et al., “H7N9 bearing a mutation in the nucleoprotein leads to increased pathology in chickens,” Frontiers in Immunology, vol. 13, 974210, 2022. DOI: https://doi.org/10.3389/FIMMU.2022.974210
[26] N. Kelvin and C. Andrew, “Effect of sex, age, diseases, and control intervention on chickens’ mortality and its financial implications in Dodoma, Tanzania,” Poultry Science, vol. 101, no. 5, 101785, 2022. DOI: https://doi.org/10.1016/J.PSJ.2022.101785
[27] S. G. M., S. Olfat, W. A. M. S., et al., “The modulatory effect of carvacrol on viral shedding titer and acute phase response in broiler chickens experimentally infected with infectious bronchitis virus,” Microbial Pathogenesis, 105410, 2022. DOI: https://doi.org/10.1016/J.MICPATH.2022.105410
[28] G. H. D., H. H., F. H. M. M., et al., “Evaluation of viral load and expression level of apoptotic genes in selected tissues of two hybrids of commercial broiler chickens challenged with infectious bronchitis virus: A comparative study,” Iranian Journal of Veterinary Research, vol. 23, no. 1, pp. 18-23, 2022. DOI: https://doi.org/10.22099/IJVR.2021.35894.5261
[29] A. Ghufran, M. Shams A. R., A. Adnan, et al., “An approach towards IoT-based predictive service for early detection of diseases in poultry chickens,” Sustainability, vol. 13, no. 23, 13396, 2021. DOI: https://doi.org/10.3390/SU132313396
[30] A. E. M. E., E. T. M., E. R. A., et al., “Necrotic enteritis in broiler chickens: Disease characteristics and prevention using organic antibiotic alternatives—a comprehensive review,” Poultry Science, vol. 101, no. 2, 101590, 2021. DOI: https://doi.org/10.1016/J.PSJ.2021.101590
[31] T. Anushri, S. Madhu, D. Amita, et al., “Pathological alterations in commercial chicken affected with salmonella infection,” Indian Journal of Veterinary Pathology, vol. 45, no. 2, pp. 109-115, 2021. DOI: https://doi.org/10.5958/0973-970X.2021.00020.1
[32] S. Mingyan, L. Chen, D. Nuo, et al., “The isolation of high-affinity ssDNA aptamer for the detection of ribavirin in chicken,” Analytical Methods, vol. 13, no. 27, 2021. DOI: https://doi.org/10.1039/D1AY00606A
[33] H. Mbelwa, J. Mbelwa, and D. Machuve, “Deep convolutional neural network for chicken diseases detection,” International Journal of Advanced Computer Science and Applications, vol. 12, no. 2, 2021. DOI: https://doi.org/10.14569/IJACSA.2021.0120295
[34] K. Hye-Ryoung, K. Yong-Kuk, J. Il, et al., “Viral metagenomic analysis of chickens with runting-stunting syndrome in the Republic of Korea,” Virology Journal, vol. 17, no. 1, 53, 2020. DOI: https://doi.org/10.1186/s12985-020-01307-z
[35] A. E. Hussein, H. M. Bejo, A. Omar, et al., “Scoring system for lesions induced by different strains of infectious bursal disease virus in chicken,” International Journal of Poultry Science, vol. 19, no. 4, pp. 153-160, 2020. DOI: https://doi.org/10.3923/ijps.2020.153.160
[36] H. R. Razooqi, A. B. Nasrullah, K. H. Shakeer, et al., “Effect of oxygenated water alone or with vaccines and antibiotics on immune response

against viral diseases and intestinal microflora community in broiler chickens," Indian Journal of Forensic Medicine & Toxicology, vol. 13, no. 4, pp. 1257-1261, 2019. DOI: https://doi.org/10.5958/0973-9130.2019.00474.2